ORIGINAL PAPER

The Evaluation of the Correlation between Radiographic Exposure Technique and Entrance Surface Air Kerma using Exposure Index from Computed Radiography

P. Kaewpookum,[a] M. Kraekratoke,[a] C. Thirinthong,[a] J. Yasamud,[a] T. Siriwiladluk,[a] P. Sisot,[a] P. Khayaiwong[a,*]

[a]Ramkhamheang University, Faculty of Science, Department of Radiological Technology, Bangkapi, Bangkok, Thailand, 10240

*Corresponding author: *Paowarin@rumail.ru.ac.th*

Received: 16 March 2019 / Revised: 15 April 2019 / Accepted: 23 April 2019

Abstract. Analog imaging systems like film-screen radiography had been gradually replaced by a digital imaging system. Computed Radiography (CR) is the most common filmless system in Thailand. However, an adjustable digital image may induce unnecessary radiation exposure to the patient. The KAP-meter, real-time transmitted dosimeter, is quite expensive when considering as the radiographic examination cost. An Exposure Index (EI). quantity derived from pixel value, is the indicator for image quality assessment used for patient dose monitoring.**:** This study aims to evaluate the correlation between radiographic exposure technique and the Entrance Surface Air Kerma (ESAK) using the EI from CR. The values of EI, ESAK, kVp, and mAs from common radiographic procedures such as skull, chest, abdomen, and pelvis were performed in anthropomorphic phantom and their correlations were analyzed by *R* (statistical data analysis software). All procedures had a strong correlation between EI and ESAK (p-value less than 0.01). Pearson's correlation coefficient (r) was 0.873, 0.901, 0.857, and 0.859 for the skull, chest, abdomen, and pelvis, respectively. There was a moderate correlation between EI and kVp in this study ($r = 0.574$, $p < 0.01$). Hence the kVp can affect the x-ray beam quality, this may alter the detective quantum efficiency (DQE) and conversion efficiency (CE) of CR. Further study of extremities radiography should be performed. The comparison between our imaging system and that of the other system may encourage dose optimization.

Keywords: Computed Radiography, Entrance surface air kerma, Exposure index, Exposure techniques

1. Introduction

Radiography is the first medical image procedure in which internal human structure can be seen noninvasively (Bradley 2008). This kind of medical image can be archived by exposed divergent x-ray photons beam transmitted patient body and projected to the image receptor. The proper radiographic image contrast depends on the variance of tissue composition and image receptor efficiency. The high atomic number (Z) material attenuates the x-ray beam greater than the low Z material. Thus, the bone is always brighter than the lung in chest radiography. Despite radiography is a noninvasive modality, the medical radiation can be induced by biological risk such as cancer (Lin 2010). The IAEA suggests the appropriate medical exposure to the patient should be performed on ALARA (As Low As Reasonably Achievable), which is the important concept of dose optimization (IAEA 2004). At the early time, a film-screen combination was the best image receptor that provided good detail of radiographic pathology. The film *optical density number* (an indicator of the gray-scale radiography) of the under-exposure image and the over-exposure image are useful visible indicators to evaluate the radiographic exposure techniques. The values for radiographic exposure technique quantities like kilovoltage-peak (kVp) refer to x-ray tube potential, mill-ampere (mA) refer to x-ray tube current, and exposure time for each radiographic procedure should be estimated the image quality and the patient doses from film-screen. However, the conventional film-screen system had been gradually replaced by either computed radiography (CR) or digital radiography (DR) system. The wide dynamic range of CR and DR and digital image processing is not only preventing over-exposure image, but also provide optimal images; for example, brightness, contrast and image size even in case of overexposure technique. Unfortunately, this may cause additional unnecessary exposure to the patient. An entrance surface air kerma (ESAK), as patient radiation dose monitoring quantity, is recommended by IAEA. There are two common methods to archived this quantity, the direct measurement using dosimeter at the patient or phantom surface and the indirect estimation calculating from x-ray tube output and simultaneous exposure technical parameters. The former need expensive dosimeter and phantom, the latter, for massive radiographic data, need the specific calculation software. An exposure index (EI) is the value related to the radiation exposure to the element of digital image receptors that can be archived without additional cost. Previous studies showed the correlation of EI and ESAK between the abdomen (Costa et al 2014) and chest (Setiewa et al 2017) procedures, but the results from patients undergoing chest digital radiography was still poor (Kaewpookum et al 2013).

This study aims to evaluate the correlation between exposure technique and the ESAK using the EI from the head, chest, abdomen, and pelvis computed radiography.

2. Materials and Methods

2.1 Material

2.1.1 The x-ray machine

Shimadzu model UD150L (Shimadzu Corporation, Kyoto, Japan). X-ray tube voltage from 40 to 150 kVp, maximum x-ray tube current of 630 mA, exposure time range available from 0.01 to 10 second and the bucky table mode.

2.1.2 The CR system

Carestream model Classic CR (Carestream Health, Inc., Rochester, NY) single-slot CR reader and the image receptors (IR) (size 24 cm * 30 cm and 35 cm * 43 cm with BaFBr: Eu^{2+} Photo-stimulated Phosphor: PSP)

2.1.3 Anthropomorphic phantom

The whole-body phantom PBU-50 (Kyoto Kagaku Co., Ltd, Kyoto, Japan) composing soft tissue and organ made from urethane-based resin and bone made from epoxy resin (**Figure 1.**)

2.1.4 The dosimeter

The air contained ionization chamber (IC) Radcal Model 10X6-6 (Radcal Corporation, CA, USA) concentric cylinder shape consists of polycarbonate walls and electrode. The 6 cm^3 active volume with conductive graphite interior coating.

Figure 1. The whole-body phantom PBU-50

2.2 Method

The determination of a correlation between the EI and the ESAK regarding the radiographic examination of the skull, chest, abdomen, and pelvis, the x-ray machine, the phantom of respective organs, the CR image receptor plate and ionization chamber were arranged (**Figure 2.**) to perform radiation dose measurement as the following

2.2.1 Exposure index (EI)

According to the dose optimization concept, the exposure technique had been trialed with consideration of the lowest radiation exposure which meets the best quality image. The best visible detail and the optimal gray-scale image of the skull, chest, abdomen, and pelvis radiography was selected. **Table 1.** shows the exposure techniques of consecutive organs that were recorded as well as their EI. The best image quality of each organ of the anthropomorphic phantom as shown in **Figure 3**. Then phantoms and image receptors were exposed by sequential divergent x-ray beams using the modified kVp and mAs as shown in **Table 2**. The full x-ray field size on IR active area was used to avoid field-size factors.

2.2.2 Entrance surface air kerma (ESAK)

The entrance surface air kerma (ESAK) of repeating x-ray exposure was measured using the ionization chamber at the level of a phantom surface with the same field size and exposure techniques (**Figure 2.**). The central ray of the x-ray beam was aligned with the sensitive volume of the IC.

2.2.3 Statistical analysis

All data were analyzed using Pearson's correlation method and 95 percent confident interval.

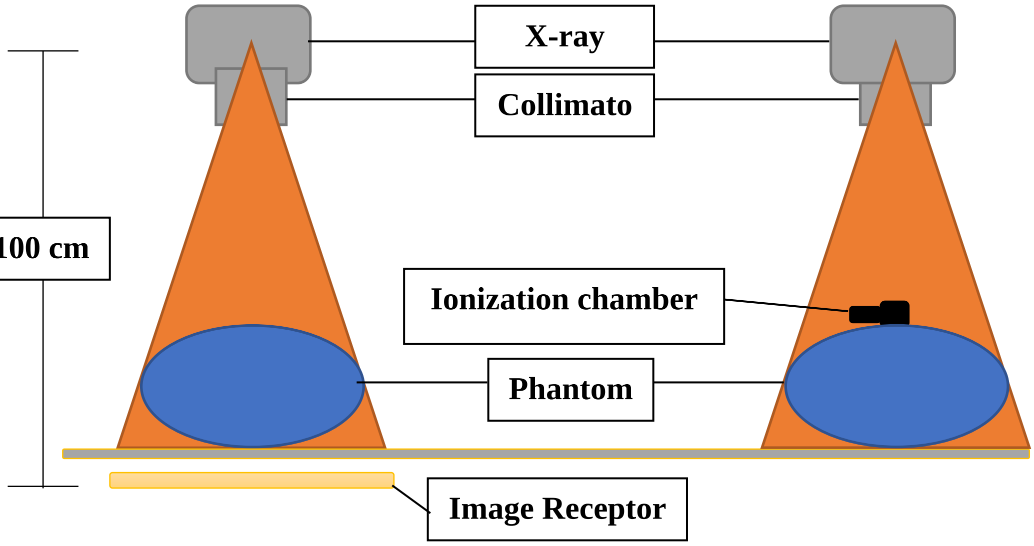

Figure 2. Geometry of dose measurement: The EI measured using image receptor (left). The ESAK measured using a cylindrical ionization chamber (right). X-ray beam (orange) projected from x-ray tube to the IR

Table 1. The appropriate exposure techniques, the ESAK (mGy), and the EI number performed on a skull, an abdomen, and a pelvic phantom.

Organs	kVp	mAs	ESAK (mGy)	EI
Skull	75	12	0.751	1696.66
Chest	85	3.2	0.327	1696.33
Abdomen	75	16	1.266	1772.33
Pelvic	75	16	1.199	1812.33

3. Results

Exposure techniques, the average ESAK, EI and Pearson's correlation coefficient (r) between the ESAK and the EI of skull, chest, abdomen, and pelvis radiography was represented in **Table 2.** The results showed the greatest ESAK of 5.052 mGy from abdomen radiography, and the smallest ESAK was 0.074 mGy from chest radiography (all radiograph was performed with an anteroposterior view). The peak tube potential was changed from 53 to 113 kV by the kVp 15%. Each organ was exposed with 100 cm source to image receptor distance (SID), except for the chest. The ESAKs were strongly correlation with the EI numbers as follows: the skull (r=0.873, p- value<0.01), the chest (r=0.901, p-value<0.01), the abdomen (r=0.875, p-value<0.01), and the pelvis (r=0.875, p=value<0.01). The EI number did not exceed the company's recommendation in each organ.

Pearson's correlation coefficient (r) among EI, ESAK, kVp, and mAs was indicated in **Table 3.** The results showed a significant correlation among EI, mAs, kVp, and ESAK as follows: EI and mAs (r=0.616), EI and kVp (r=0.574), ESAK and mAs (r=0.957), and EI, kVp and mAs (r=0.955). There was no correlation between ESAK and kVp (r=0.052, p-value =0.763).

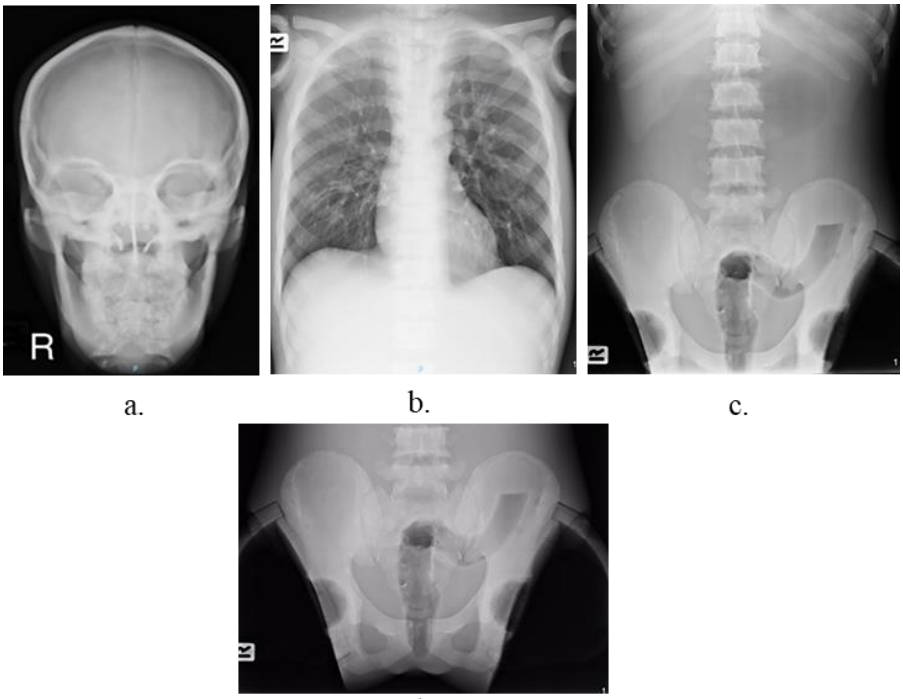

Figure 3. Radiography of skull (a.), chest (b.), abdomen (c.), pelvis (d.)

Table 2 Exposure techniques, the average ESAK, EI and Pearson's correlation coefficient (r) between the ESAK and EI of skull, chest, abdomen, and pelvis radiography

Organs	Exposure technique			ESAK (mGy)	EI	ESAK and EI correlation coefficient	
	kV	mAs	SID (cm)			r	p-value
Skull	54	12	100	0.378	1203	0.873	<0.01
	64	12	100	0.550	1463		
	75	3.2	100	0.193	1184		
	75	6.3	100	0.379	1435		
	75*	12*	100	0.751	1697		
	75	50	100	3.036	2265		
	86	12	100	0.977	1886		
	99	12	100	1.286	2081		
Chest	61	3.2	133	0.074	1302	0.901	<0.01
	72	3.2	133	0.106	1499		
	85	0.8	133	0.045	1274		
	85	1.6	133	0.080	1486		
	85*	3.2*	133	0.147	1697		
	85	6.3	133	0.286	2009		
	85	12	133	0.565	2263		
	98	3.2	133	0.194	1901		
	113	3.2	133	0.254	2046		
Abdomen	53	16	100	0.608	1162	0.857	<0.01
	62	16	100	0.874	1454		
	75	4	100	0.320	1192		
	75	8	100	0.628	1459		
	75*	16*	100	1.266	1772		
	75	32	100	2.503	2057		
	75	63	100	5.052	2346		
	86	16	100	1.612	1983		
	99	16	100	2.142	2173		
Pelvis	53	16	100	0.586	1253	0.859	<0.01
	62	16	100	0.832	1549		

Organs	Exposure technique			ESAK (mGy)	EI	ESAK and EI correlation coefficient	
	kV	mAs	SID (cm)			r	p-value
	75	4	100	0.308	13250		
	75	8	100	0.605	1598		
	75*	16*	100	1.199	1812		
	75	32	100	2.415	2141		
	75	63	100	4.859	2414		
	86	16	100	1.563	2061		
	99	16	100	2.039	2232		

**The exposure techniques of the smallest ESAK among the best image quality group*

Table 3 The Pearson's correlation coefficient of testing parameter

Testing Parameters	Pearson's correlation coefficient	
	r	p-value
EI and mAs	0.616	<0.01
EI and kVp	0.574	<0.01
ESAK and kVp	0.052	0.763
ESAK and mAs	0.957	<0.01
EI, kVp and mAs	0.955	<0.01

4. Discussion

In this study, the image quality of CR was achieved by assessing the following factors. First, correcting the organ positioning and collimating to meet the acceptable image contrast. Then, optimizing the exposure technique of each organ using the vendor indicators as the key to perform a proper exposure to image receptor (exposure index, for example). After that, selecting an appropriated image processing algorithm for each organ of interest. Finally, ensuring that none of image artifact had been seen (Pongnapang 2005).

The publication (Costa et al 2014) reported the manually extracted EI at the time of image processing was strongly correlated to ESAK which been established indirectly calculated from incident air kerma measured by parallel chamber and recorded exposure techniques of patients undergoing abdomen radiography. Recent~~ly~~ report (Setiewan et al 2017) also showed a strong correlation between ESAK derived from EI and calculated ESAK based on RaySaftX2 dosimeter measuring in ANSI phantom and chest radiographic exposure technique ($r = 0.819$, p-value < 0.01). On the other hand, the correlation between EI and ESAK derived from KAP-meter ($r = 0.2$) in patients undergo chest digital radiography was poor (Kaewpookum et al 2013). Nonetheless, our study, suggests that the correlation coefficients of exposure index in four parts of radiographic examinations is a strongly significant correlated with ESAK. Moreover, our report also corresponds to the trend that an EI is proportional to ESAK and exposure techniques (Seibert 2011),.

The result showed ESAK and kVp were not correlated because kVp affected to both beam quality and quantity. Beam quality parameters such as kVp and half-value layer (HVL) should be determined before the measurement of ESAK, according to Technical report series number 457 (IAEA 2007). When we considered other parameters, we found that the correlation coefficient of EI and kVp was moderated because kVp was related to x-ray beam penetrating power. High x-ray transmission and scatter radiation is influenced by the increasing of kVp, therefore, the rising of signal and noise absorption into IR are described by the raise in the remnant radiation (transmitted and scattered radiation). After the absorption, the electronic signal is converted and changed to a digital image. The effectiveness of absorption and conversion signal is evaluated by the detective quantum efficiency (DQE) and conversion efficiency (CE). Both DQE and CE might be changed after altering kVp. Also, the quality of image is related to scattered radiation and ~~it~~ depends on remnant x-ray photons (Naji et al 2017). An EI value estimates the digital signal level from the patient's transmission radiation and signal-to-noise ratio, and image quality assessment. Several CR systems recommend the kVp number for various parts of radiographic examinations (Seibert 2011).

Although the EI is related to ESAK, the EI still cannot replace the standard patient dosimeter. We notice~~d~~ that there are four factors must be considered before applying EI in the clinical radiographic procedure. First, there is the use of anthropomorphic phantom instead of the patient. A phantom has a rigid internal structure while the patient body part has anatomical variation and movement. Second, distances between the x-ray source and two detectors (IC and image plate) are different. The patient dose is not directly calculated by using EI number, it is an idea to select the suitable exposure technique which is important to optimize radiation doses to the patient (Seibert 2011). For this test, the SID of the chest was 133 cm instead of 180 cm due~~s~~ to the x-ray tube height limit. The mAs cannot be adjusted finely because of the x-ray generator limitation. Third, ESAK is measured as a point dose, but EI is derived from planar pixel value. The size of the IC is larger than the detector in IR because there is not the smallest size detector which is equal to the diameter of the IR detector. Finally, ESAK is measured at the phantom's surface (without attenuator) while EI is derived from the exposure to the image detector due to transmitted x-ray at the level of image plate (with attenuator). Therefore, the ESAK, referred to as any point on skin of a patient, is the same radiation dose, but EI is estimated in all areas of the field of interest. Both EI and ESAK are used for radiation dose assessment for this study.

Even we cannot use the EI as the standard dosimeter, we can use it for the dose monitoring tool. Radiological technologists who familiar with the EI and ESAK relationship could optimize exposure to the patient undergo CR as well as the basis of over-exposure image in the film-screen system. In some radiology departments that did not have the sophisticated dosimeter like KAP meter or expensive anthropomorphic phantom, the EI is one of the indicators for the dose monitoring.

5. Conclusion

For this study, a strong correlation between exposure technique and ESAK is revealed. An EI of computed radiography system acts as the useful dose monitoring indicator without additional costs. Further study of extremities radiography should be performed. The comparison between our imaging system and other commercial systems may encourage dose optimization.

Acknowledgments

This study cannot be succeeded unless the attentive support from department of Radiological Technology, Faculty of Science, Ramkhamheang University

References

Bradley WG (2008) History of medical imaging. Proceeding of the American Philosophical Society 152(3):349-361

Costa AM, Pelegrino (2014) Evaluation of entrance surface air kerma from exposure index in computed radiography. Radiation Physics and Chemistry 104:198-200

Internal Atomic Energy Agency, IAEA (2004) Optimization of the radiological protection of patients undergoing radiography, fluoroscopy and computed tomography IAEA-TECDOC-1423. IAEA, Vienna

International Atomic Energy Agency, IAEA (2007) Dosimetry in diagnostic radiology: an international code of practice Technical report series no. 457. IAEA, Vienna

Kaewpookum P, Pongnapang N, Saengruang-Orn S (2013) Correlations among Entrance Surface Air KERMA, KERMA-Area Product and Exposure Index in Chest Digital Radiography at

Phramongkutklao Hospital. Royal Thai Army Medical Journal 66:103-109

Lin EC (2010) Radiation Risk from Medical Imaging. Mayo Clin Proc 85(12):1142-1146

Naji AT, Jaafar MS, Ali EA, Al-Ani SKJ (2017) Effect of Backscattered Radiation on X-ray Image Contrast. Applied Physics Research 9(1):105-114

Pongnapang N (2005) Practical guidelines for radiographers to improve computed radiography image quality. Biomed Imaging Interv J 1(2): e12

Seibert JA, Motin RL (2011) The standardized exposure index for digital radiography: an opportunity for optimization of radiation dose to the pediatric population. Pediatr Radiol 41:573-581

Setiawan AN, Suryono, Hadisaputro S, Santoso AG, Santoso B, Sugiyanto, Wibowo GM (2017) Exposure Index and Entrance Surface Dose of ANSI Chest Phantom with Computed Radiography. Int J of Allied Med Sci and Clin Research 5(4):947-953